Power System Resilience Enhancement in Typhoons Using a Three-Stage Day-Ahead Unit Commitment

Tao Ding, *Senior Member, IEEE*, Ming Qu, *Student Member, IEEE*, Zekai Wang, *Student Member, IEEE*, Bo Chen, *Member, IEEE*, Chen Chen, *Senior Member, IEEE*, and Mohammad Shahidehpour, *Life Fellow, IEEE*

***Abstract*—We propose a three-stage resilient unit commitment model which considers uncertain typhoon paths and line outages to improve the power system resilience against typhoon events. The proposed solution coordinates resources in response to the worst-case scenario for each possible typhoon path. The optimal decision is based on the characterization of the power system schedule into three stages of preventive control, emergency control, and restoration. Preventive control is performed before the typhoon occurs by quickly adjusting the three-stage resilient unit commitment schedule; emergency control is conducted during the typhoon by shedding local loads to meet the power balance, while other control strategies are assumed to be unavailable due to possible interruptions in the communication system; restoration is realized after the typhoon, when resources are optimally dispatched to repair the outages of critical devices and recover the normal operation state of the power system quickly. Considering the typhoon path uncertainty, we have introduced a stochastic model for possible typhoon paths where all possible affected lines along each typhoon path are assumed to be on outage during the typhoon. Accordingly, we explore the strategy for co-optimizing the three stages in unit commitment. The proposed model is tested on the IEEE 118-bus system and the real-world provincial system to verify its effectiveness.**

***Index Terms*—Typhoon, resilience, power system restoration, three-stage resilient unit commitment.**

I. Introduction

POWER systems are cornerstones of modern societies. The importance of the power system has promoted the notion of mitigating blackouts expeditiously and maintaining necessary power supplies as extreme conditions evolve. However, recent accidents caused by extreme events resulted in major social losses, revealing that the current power system hierarchies are still vulnerable to extreme events.

Manuscript received April 22, 2020; revised August 29, 2020 and November 17, 2020; accepted December 26, 2020. Date of publication December 30, 2020; date of current version April 21, 2021. This work was supported in part by the National Natural Science Foundation of China under Grant 51977166; in part by the China Postdoctoral Science Foundation under Grant 2017T100748; and in part by the Natural Science Foundation of Shaanxi Province under Grant 2020KW-022. Paper no. TSG-00576-2020. *(Corresponding author: Mohammad Shahidehpour.)*

Tao Ding, Ming Qu, Zekai Wang, and Chen Chen are with the Department of Electrical Engineering, Xi'an Jiaotong University, Xi'an 710049, China.

Bo Chen is with the Energy Systems Division, Argonne National Laboratory, Lemont, IL 60439 USA.

Mohammad Shahidehpour is with the ECE Department, Illinois Institute of Technology, Chicago, IL 60616 USA (e-mail: ms@iit.edu).

Color versions of one or more figures in this article are available at https://doi.org/10.1109/TSG.2020.3048234.

Digital Object Identifier 10.1109/TSG.2020.3048234

In 2008, a major ice storm in Southern China caused more than 451-line outages in which 14.66 million consumers were impacted by this disaster [1]. In 2011, a Japanese tsunami resulted in power outages which lasted over 7 days and involved more than 4 million consumers [2]. In 2015, the Ukrainian power grid was hacked, resulting in power outages affecting approximately 225,000 customers for several hours [3]. In 2017, a blackout in Taiwan occurred due to human errors and lack of sufficient reserve capacity, in which 6.68 million consumers were affected by power outages [4]. As the climate deteriorates, the frequency of extreme events will also increase significantly. Between 2018-2015, the number of power outrage events caused by extreme weather has increased 64% in the U.S., with Huge economic losses [5].

Many scholars have carried out a great deal of research on assessing power system resilience that would address the related problems in power system planning and operation. Reference [6] presented the definition of a resilient power system and introduced three stages, including resist and absorb, response and adapt, and recovery from outages. In addition, a qualification method was proposed for resilience and some strategies were carried out to improve the power system resilience. Reference [7] presented the concept of resilience for critical infrastructure systems and a corresponding resilience assessment methodology was proposed, which characterized the threats by their various consequences. A novel resilience quantification framework was introduced in [8] to interpret the concept of infrastructure resilience by using different resilience indicators. Reference [9] presented a strategy and framework for the coupled systems of urban traffic and power distribution. The system recovery capability was improved through line hardening and distributed generation planning when power outages occur in power distribution network and traffic signals. References [10], [11] focused on the definition of power system resilience, reviewed key concepts, and paved the way for the creation of appropriate and effective resilience standards, measures, and indices.

Some scholars have advocated a higher resilience in power systems by introducing new types of equipment and energy storage devices. An integrated resilience response (IRR) framework was proposed in [12] to enhance the power grid resilience against natural disasters. IRR was proved to be preferable to both independent preventive and corrective responses. Moreover, topology switching in the integrated resilience response strategy also was able to enhance power

grid resilience. Reference [13] studied a four-loop switching controller for a doubly fed induction generator to improve the resilience of wind-power penetrated power systems. The study proved that the four-loop switching controller could show greater robustness to extreme disturbances. Because the underground natural gas system was considered less vulnerable than the power system to extreme events, an integrated electricity and natural gas transportation system planning system was proposed to enhance the power system's resilience in [14]. Reference [15] set up a dispatch model for combined heat and power systems considering the heat transfer and storage processes, and proved that a hybrid system of heat and electricity could feasibly provide a black-start power source, although the cost was relatively higher than that of a PV station. A defense optimization model was proposed in [16] for strengthening the critical lines on a shipboard power system, so that the load shedding from the deliberate attacks could be mitigated. Undeniably, enhancing the power system hardware can significantly improve the system resilience. Meanwhile, advanced power system equipment introduced the foundation for realizing intelligent control algorithms in a smart grid.

Moreover, some scholars combined power systems with machine learning and big data technologies to improve the grid resilience. Reference [17] used machine learning to address the multivariate effects on the power system resilience in order to predict resilience under random disturbances. Reference [18] used big data methods to analyze distribution power system data from phasor measurement units to study the security and flexibility of power systems. The authors also proposed another two real world cases for remote asset monitoring and distribution-level oscillation analyses.

It is critical to model extreme weather cases before analyzing power system resilience under natural disasters. A Markov model was proposed in [19] to construct sequentially proactive generation dispatch strategies considering operating constraints, which took into account the uncertainty of extreme events and could reduce load curtailments through proactive operations. The authors established a fragility model to assess storm effects moving across a transmission network. Furthermore, [20] described and demonstrated a probabilistic method to assess and evaluate adaptation measures against extreme weather cases. However, recovery strategies required greater flexibility due to the uncertain nature of extreme weather forecasting. Reference [21] proposed a resilience enhancement strategy for power transmission system against ice storms. This article used a two-stage robust optimization model to accommodate a variable ice thickness on transmission lines. Reference [22] set up a multi-stage VAR planning model considering various defensive and restorative resilience metrics to assess the voltage performance and improve the voltage stability.

In addition, some scholars considered optimization models with diverse control devices to improve the power grid resilience. Reference [23] regarded the restoration process as an optimization problem with temporal constraints, which schedules generator start-ups. Reference [24] used four heuristic algorithms to represent state variables and initial sub-optimal generation states in a solution space with promising results for typical distribution networks. References [25]–[32] focused on the resilience enhancement for distribution networks by Markov decision process, crew dispatch, distributed generators, network reconfiguration, optimal planning and intended microgrids.

The problem of *N-k* unit commitment has also received much attention. It was indicated in [33] that the Federal Energy Regulatory Commission incorporated ancillary service demand response programs into the *N-k* unit commitment problem to reduce extreme outage impacts on power grids. The model was formulated as a mixed-integer programming problem. Reference [34] proposed a double-layer robust method to solve the contingency-constrained single-bus unit commitment problem with security criteria and generation unit outages. Moreover, all component outage scenarios were considered in a robust model to solve the N-k contingency-constrained unit commitment in [35]. References [36] and [37] studied the unit commitment schedule for the day-ahead market with *N-k* constraints. Unlike the previously mentioned references, these papers developed an α-quantile measurement method to address wind power generation and demand forecasted errors in a chance-constrained optimization problem.

Generally, a resilient power system should consider all three stages stated simultaneously [6]. However, most of the previous optimization models focused on a single stage or two stages. For example, a resilient unit commitment problem was formulated as a two-stage robust optimization model in [38] which considered both prevention and emergency stages. However, the repair process was simply considered as an automatic repair within a certain period of time after line outages, without considering the repair resource allocation strategies. However, the limited repair resources do impact the restoration stage and, by extension, prevention and emergency controls. For example, if some critical lines can be repaired in time for weak areas, some critical loads can be picked up and the original backups for these weak areas can be shifted to other areas.

In this article, we explore the strategy for co-optimizing the three stages in unit commitment. The main contributions of this article are summarized as follows.

(i) A resilient unit commitment is proposed to coordinate the three stages. Specifically, preventive control in each area will adjust the generation dispatch or the unit commitment schedule to cope with the coming natural disasters; emergency control is conducted during the typhoon by applying a local load curtailment to meet the power balance as soon as possible; and restoration is applied to each area after the typhoon event in which case available resources are optimally dispatched to repair critical components.

(ii) The power network is dynamically divided into four sections with three stages to quantify the power system resilience, where preventive control, emergency control, and restoration are performed in each bus and transmission line. It is challenging to obtain the line outage probability in typhoons and other infrequent and extreme events. Therefore, to fully guarantee the power system security considering the typhoon path uncertainty, we have introduced a stochastic model for possible

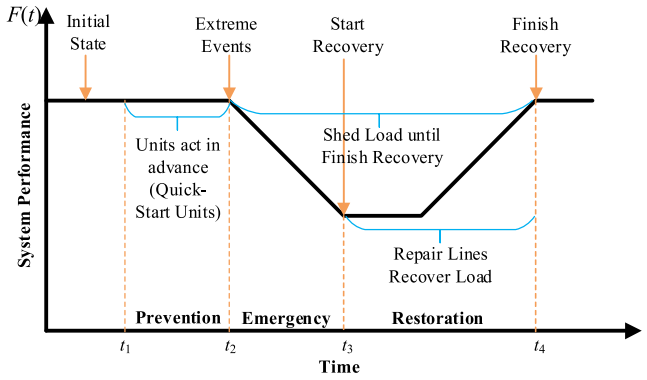

Fig. 1. Power system resilience.

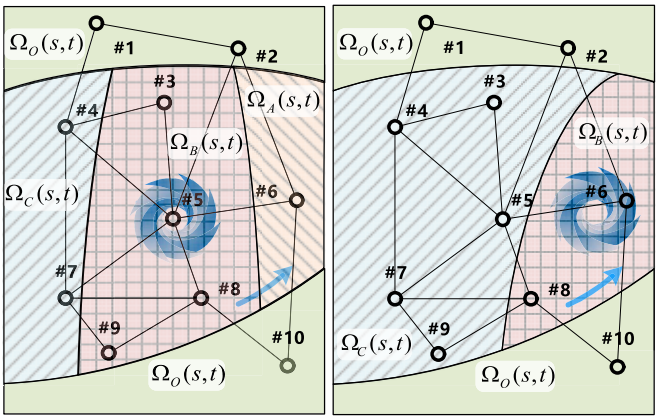

Fig. 2. Four dynamic sets of buses/lines during a typhoon.

typhoon paths where all lines along each typhoon path are assumed to be on outage during the typhoon so that the proposed resilient unit commitment can protect the power grid against the worst-case scenario.

The remainder of this article is organized as follows. Section II defines power system resilience and gives the modeling of the resilient unit commitment. In Section III, numerical results and comparisons on both small and large-scale test systems verify the effectiveness of the proposed method. Conclusions are drawn and future works are delineated in Section V.

II. Three-Stage Resilient Unit Commitment Model

A. Modeling of Power System Resilience and Dynamic Sets

Traditionally, power systems rely on probability-based reliability evaluation or risk assessment methods to evaluate outage conditions. The key power system elements are hardened or expanded accordingly to maintain safe and stable operation margins in extreme events, such as natural disasters. However, unlike reliability evaluation or risk assessment methods, resilience measure and enhancement methods represent dynamic processes that could flexibly adjust power system resources to cope with extreme events.

In response to unavoidable natural disasters, the entire process of maintaining a resilient power system can be generalized into three stages as depicted in Fig. 1. These stages are presented as follows.

(1) Preventive control: Before a natural disaster occurs, preventive control should be performed based on the prior forecasting information against the potential natural disasters. For example, it is necessary to adjust the generation scheduling or change the fast-start unit commitment to cope with the coming natural disasters.

(2) Emergency control: During natural disasters, the system dynamically responds to withstand severe disturbances and prevent further collapse. Because the communication system may be interrupted at this time, the emergency control strategies only consider local load curtailment to guarantee the power balance as soon as possible.

(3) Restoration: After natural disasters, the system can quickly return to its normal status by optimally scheduling resources to repair critical devices (e.g., transmission lines, transformers), and reconfiguring the network topology to minimize total load curtailment.

Since natural disasters may have different characteristics, this article will focus its study on typhoon events. Generally, during a typhoon event, power grid buses/lines are divided into four dynamic sets:

1) Bus set $\Omega_A(s,t)$/line set $\Omega_A^l(s,t)$: buses/lines in $\Omega_A(s,t)$/ Ω_A^l (s,t) is within the typhoon path and the typhoon has not arrived here yet at time period t for s-th path;

2) Bus set Ω_B (s,t) / line set $\Omega_B^l(s,t)$: buses/lines in Ω_B (s,t) /$\Omega_B^l(s,t)$ is within the typhoon path and is during the event at time period t for s-th path;

3) Bus set Ω_C (s,t) / line set $\Omega_C^l(s,t)$: buses/lines in Ω_C (s,t) /$\Omega_C^l(s,t)$ is within the typhoon path and the typhoon has left here at time period t for s-th path;

4) Bus set $\Omega_O(s,t)$ and line set $\Omega_O^l(s,t)$: buses/lines in Ω_O (s,t) / Ω_O^l (s,t) is outside the typhoon path and is not affected by the typhoon in the entire dispatching period t for s-th path.

Consider a case in Fig. 2 for illustration, where a typhoon moves from the left to the right. At the time t_n for s-th path, the above sets are given as $\Omega_A(s,t_n) = \{6\}$, $\Omega_B(s,t_n) = \{3, 5, 8, 9\}$, $\Omega_C(s,t_n) = \{4, 7\}$, $\Omega_O(s,t_n) = \{1, 2, 10\}$, $\Omega_A^l(s,t_n) = \{2\text{-}6, 6\text{-}10\}$, $\Omega_B^l(s,t_n) = \{2\text{-}5, 3\text{-}4, 3\text{-}5, 4\text{-}5, 5\text{-}6, 5\text{-}7, 5\text{-}8, 7\text{-}8, 7\text{-}9, 8\text{-}9, 8\text{-}10\}$, $\Omega_C^l(s,t_n) = \{1\text{-}4, 4\text{-}7\}$, $\Omega_O^l(s,t_n) = \{1\text{-}2\}$. After several periods, e.g., t_{n+k}, all the sets will be changed to $\Omega_A(s,t_{n+k}) = \varnothing$, $\Omega_B(s,t_{n+k}) = \{6, 8\}$, $\Omega_C(s,t_{n+k}) = \{3, 4, 5, 7, 9\}$, $\Omega_O(s,t_{n+k}) = 1, 2, 10$, $\Omega_A^l(s,t_{n+k}) = \varnothing$, $\Omega_B^l(s,t_{n+k}) = \{2\text{-}6, 5\text{-}6, 8\text{-}8, 6\text{-}10, 7\text{-}8, 8\text{-}9, 8\text{-}10\}$, $\Omega_C^l(s,t_{n+k}) = \{1\text{-}4, 3\text{-}4, 3\text{-}5, 4\text{-}5, 4\text{-}7, 5\text{-}7, 2\text{-}5, 7\text{-}9\}$, $\Omega_O^l(s,t_{n+k}) = \{1\text{-}2\}$.

It is found that three-stage resilient unit commitment is a critical component of the proposed method to cope with typhoon events. Since generators on the typhoon path will be triggered, fast-start units considered in preventive control can be committed in place of units on the future typhoon path, so that the load shedding can be mitigated. On the other hand, unit commitment and line repair should be coordinated to recover the critical load in the restoration process. Therefore, we propose a three-stage resilient unit commitment model for day-ahead to optimize a power system schedule that incorporates the control strategies in the stated three stages by using the above proposed dynamic sets. Note that these dynamic

TABLE I
FLOWCHART OF THE THREE-STAGE RESILIENT UNIT COMMITMENT

Input	Typhoon information and network parameters
Output	Three-stage resilient unit commitment solution
Step 1	for s=1:N_s
Step 2	for t=1:T
Step 3	Determine the worst-case scenario and Generate the sets $\Omega_A(s,t)$, $\Omega_B(s,t)$, $\Omega_C(s,t)$, $\Omega_o(s,t)$, $\Omega^l{}_A(s,t)$, $\Omega^l{}_B(s,t)$, $\Omega^l{}_C(s,t)$ and $\Omega^l{}_o(s,t)$
Step 4	switch (sets):
Step 5	case $\{\Omega_A(s,t), \Omega^l{}_A(s,t)\}$:
Step 6	Add constraints ①②③④⑤⑥
Step 7	Break
Step 8	case $\{\Omega_B(s,t), \Omega^l{}_B(s,t)\}$:
Step 9	Add constraints ②③⑤
Step10	Break
Step11	case $\{\Omega_C(s,t), \Omega^l{}_C(s,t)\}$:
Step12	Add constraints ①②③④⑤⑥⑦
Step13	Break
Step14	case $\{\Omega_o(s,t), \Omega^l{}_o(s,t)\}$:
Step15	Add constraints ①②③④⑤⑥
Step16	Break
Step17	End
Step18	End
Step19	End
Step20	Solve the unit commitment model

sets of buses/lines are closely tied to typhoon forecasts with the help of sophisticated forecasting techniques such as a geographic information system. However, an accurate typhoon path forecast is still challenging. To fully guarantee the power system security considering the typhoon path uncertainty, we have introduced a stochastic model for possible typhoon paths where all lines along each typhoon path are assumed to be on outage during the typhoon so that the proposed three-stage resilient unit commitment can protect the power grid against the worst-case scenario.

Generally, the three-stage resilient unit commitment includes seven constraint sets: ① logic constraint; ② power flow constraint; ③ generator dispatch constraint; ④ generator ramping rate constraint; ⑤ generator up/down time constraint; ⑥ spinning reserve constraint; ⑦ resource management constraint. The flowchart of the proposed three-stage resilient unit commitment can be found in Table I. Specifically, all the units connected to the buses in $\Omega_A(s,t)$ and $\Omega_O(s,t)$ can be scheduled, so constraints ①-⑥ need to be considered. The units connected to the bus in $\Omega_B(s,t)$ cannot be scheduled and should maintain the original operating states, so only constraints ②③⑤ are needed. The units connected to the buses in $\Omega_C(s,t)$ can be scheduled. In addition, since the typhoon has left and the communication system has been restored, line repair constraint ⑦ is considered, besides the constraints ①-⑥.

B. Objective Function of Resilient Unit Commitment

The objective is to minimize the total expected outage cost during the dynamic process with physical and temporal power system constraints considering the worst-case scenario for all possible typhoon paths. The proposed mathematical formulation is expressed as

$$\min \sum_{s=1}^{N_s} \rho_S \sum_{t=1}^{T} \left\{ \underbrace{F_{s,t}^{\text{pre}}}_{\text{before}} + \underbrace{F_{s,t}^{\text{during}}}_{\text{during}} + \underbrace{F_{s,t}^{\text{post}}}_{\text{after}} + \underbrace{F_{s,t}^{\text{other}}}_{\text{other}} \right\} \tag{1}$$

where T is the total number of periods; $F_{s,t}^{\text{pre}}$, $F_{s,t}^{\text{during}}$, $F_{s,t}^{\text{post}}$, and $F_{s,t}^{\text{other}}$ are the four-area cost functions at time t for s-th path. N_s is the total number of possible typhoon paths. ρ_s is the probability for s-th typhoon path.

Before the typhoon event, the preventive schedule of generation units will satisfy physical constraints. Accordingly, certain critical units will alter their commitment schedules to mitigate any load curtailment should a typhoon event occur. Thus, the adjusted objective function is expressed as

$$F_{s,t}^{\text{pre}} = \sum_{i \in \Omega_A(s,t) \bigcap \Omega_G} \Big(a_i P_{G,i,s,t}^2 + b_i P_{G,i,s,t} + c_i x_{G,i,t} + C_i^{\text{UP}} v_{G,i,t} + C_i^{\text{DN}} w_{G,i,t} \Big) \tag{2}$$

where (a_i, b_i, c_i) are the cost coefficients for unit i; $x_{G,i,t}$ is the commitment state of unit i at time t; $x_{G,i,t} = 1$ if the unit is in operation, and $x_{G,i,t} = 0$ otherwise; $P_{G,i,s,t}$ is the active power output of unit i at time t for s-th path; C_i^{UP} and C_i^{DN} are start-up and shut-down costs of unit i at time t; $v_{G,i,t}$ and $w_{G,i,t}$ are start-up and shut-down states of unit i at time t; $v_{G,i,t}, w_{G,i,t} = 1$ if the unit i starts up or shuts down at time t, and $v_{G,i,t}, w_{G,i,t} = 0$ otherwise; j is the index of load bus; O_G is the set of generators.

Note that the communication system may be on outage within an affected area such that generation units cannot be deployed during this period. Accordingly, local load curtailment is used to guarantee the power balance. Thus, the cost function is stated as

$$F_{s,t}^{\text{during}} = \sum_{i \in \Omega_B(s,t) \bigcap \Omega_G} M_{G,i} \big(v_{G,i,t} \vee w_{G,i,t} \big) + \sum_{j \in \Omega_B(s,t)} \gamma_j \Delta P_{L,j,s,t} \tag{3}$$

where $M_{G,i}$ is the penalty coefficient to prevent any commitment since the unit cannot be deployed; $\vee$ is the "or" operator; γ_j is the load cost at bus j at time t; $\Delta P_{L,j,s,t}$ is the load curtailment of bus j at time t for s-th path during a typhoon event. The first term is to prevent unit commitment in this area and the second term is to realize load curtailment to balance the power. Furthermore, the "or" operator in (3) can be exactly linearized by introducing a dummy binary variable $\delta_{G,i,t}$ and then reformulated as

$$F_{s,t}^{\text{during}} = \sum_{i \in \Omega_B(s,t) \bigcap \Omega_G} M_{G,i} \delta_{G,i,t} + \sum_{j \in \Omega_B(s,t)} \gamma_j \Delta P_{L,j,s,t} \tag{4}$$

with the additional constraints

$$\delta_{G,i,t} \geq v_{G,i,t}, \delta_{G,i,t} \geq w_{G,i,t}, \delta_{G,i,t} \leq v_{G,i,t} + w_{G,i,t} \tag{5}$$

Next, the goal is to implement the power system recovery by quickly repairing the critical components that are on

outage. The corresponding objective function includes three parts which are: generation cost, load curtailment and repair cost, such that

$$F_{s,t}^{\text{post}} = \sum_{i\in\Omega_C(s,t)\bigcap\Omega_G}\Big(a_iP_{G,i,s,t}^2 + b_iP_{G,i,s,t} + c_ix_{G,i,t} + C_i^{\text{UP}}v_{G,i,t} + C_i^{\text{DN}}w_{G,i,t}\Big) + \sum_{j\in\Omega_C(s,t)}\gamma_j\Delta P_{L,j,s,t} + \sum_{l\in\Omega_C^l(s,t)}C_l^{REP}z_{l,s,t} \quad (6)$$

where C_l^{REP} is the repair cost for the l-th line on outage; $z_{l,s,t}$ is the line l repair state at time t for s-th path. $z_{l,s,t} = 1$ if line l is being repaired; otherwise, $z_{l,s,t} = 0$. The unit commitment of all units and load curtailment are coordinated in areas which are not affected by the typhoon to guarantee the power balance,

$$F_{s,t}^{\text{other}} = \sum_{i\in\Omega_O(s,t)\bigcap\Omega_G}\Big(a_iP_{G,i,s,t}^2 + b_iP_{G,i,s,t} + c_ix_{G,i,t} + C_i^{\text{UP}}v_{G,i,t} + C_i^{\text{DN}}w_{G,i,t}\Big) + \sum_{j\in\Omega_O(s,t)}\gamma_j\Delta P_{L,j,s,t} \quad (7)$$

C. Three-Stage Resilient Unit Commitment Constraints

Since dynamic sets are changed in each period, the unit commitment constraints will be formulated for each dynamic set at each period.

1) Logic Constraint: Logic constraints show the relationship between the unit state $x_{g,i,t}$ and the start-up/shut-down $(v_{G,i,t}, w_{G,i,t})$ state. If a unit starts up at time t, then $x_{G,i,t} = 1$ and $v_{G,i,t-1} = 0$, which leads to $v_{G,i,t} = 1$; otherwise, $v_{G,i,t} = 0$. Similarly, if the unit shuts down at time t, then $x_{g,i,t} = 0$ and $x_{g,i,t-1} = 1$, which leads to $w_{G,i,t} = 1$; otherwise $w_{G,i,t} = 0$. The above logic expression is formulated as

$$x_{G,i,t} - x_{G,i,t-1} = v_{G,i,t} - w_{G,i,t}, v_{G,i,t} + w_{G,i,t} \le 1 \quad \forall i \in \Omega_G\bigcap\Big(\Omega_A(s,t)\bigcup\Omega_C(s,t)\bigcup\Omega_O(s,t)\Big), \quad \forall t \in [1,T] \quad \forall s \in [1,N_s] \quad (8)$$

2) Power Flow Constraint: In typhoons, generation unit dispatch can be adjusted and the load demand may be curtailed to guarantee the bus power balance at each period. In this article, a linear power flow model is employed, where

$$P_{G,i,s,t} - \Big(P_{L,i,t}^0 - \Delta P_{L,i,s,t}\Big) = \sum_{\forall j\in\Omega_N}F_{ij,s,t}, \quad \forall i \in \Omega_N \quad \forall t \in [1,T] \quad \forall s \in [1,N_s] \quad (9)$$

$$Q_{G,i,s,t} - \Big(Q_{L,i,t}^0 - \Delta Q_{L,i,s,t}\Big) = \sum_{\forall j\in\Omega_N}Q_{ij,s,t}, \quad \forall i \in \Omega_N \quad \forall t \in [1,T] \quad \forall s \in [1,N_s] \quad (10)$$

$$\theta_{ref,t} = 0 \quad \forall t \in [1,T] \quad (11)$$

where Ω_N is the set of power system buses; $F_{ij,s,t}$ and $Q_{ij,s,t}$ are active and reactive power flows from bus i to bus j at time t for s-th path; $P_{L,i,t}^0$ and $Q_{L,i,t}^0$ are the normal active and reactive load demands of bus i at time t; $Q_{G,i,s,t}$ is the reactive power output of unit i at time t for s-th path; $\Delta Q_{L,i,s,t}$ is the reactive load curtailment of bus i at time t for s-th path; $\theta_{ref,t}$ is the angle of the reference bus at time t.

The active and reactive power flows are expressed as

$$F_{ij,s,t} = \Big(G_{ij}V_{j,s,t} - B'_{ij}\theta_{j,s,t}\Big)y_{l,s,t}, \quad \forall l = (i,j) \in \Omega_L \quad \forall t \in [1,T] \quad \forall s \in [1,N_s] \quad (12)$$

$$Q_{ij,s,t} = \Big(B_{ij}V_{j,s,t} - G'_{ij}\theta_{j,s,t}\Big)y_{l,s,t}, \quad \forall l = (i,j) \in \Omega_L \quad \forall t \in [1,T], \forall s \in [1,N_s] \quad (13)$$

$$V_j^{\min} \le V_{j,s,t} \le V_j^{\max} \quad \forall i \in \Omega_N \quad \forall t \in [1,T] \quad \forall s \in [1,N_s] \quad (14)$$

$$\begin{cases} -F_l^{\max} \le F_{ij,s,t} \le F_l^{\max} \\ -F_l^{\max} \le Q_{ij,s,t} \le F_l^{\max}, \end{cases} \quad \forall l = (i,j) \in \Omega_L, \forall t \in [1,T], \forall s \in [1,N_s] \quad (15)$$

where G_{ij} and B_{ij} are real and imaginary parts of admittance matrix, respectively; $G_{ij}{}'$ and $B_{ij}{}'$ are real and imaginary parts of admittance matrix without shunt elements, respectively; $V_{j,s,t}$ and $\theta_{j,s,t}$ are voltage magnitude and angle of bus i at time t for s-th path, respectively; $y_{l,s,t}$ is the state of the l-th transmission line at time t for s-th path; $y_{l,s,t} = 1$, if the line is in service and $y_{l,s,t} = 0$, otherwise; O_L is the set of transmission lines; F_l^{max} is the maximum allowable power flow on line (i, j). V_j^{min} and V_j^{max} are the minimum and the maximum voltage magnitude limits of bus j. Then, the bilinear term in (12) and (13) can be linearized as

$$\begin{cases} -y_{ij,s,t}F_l^{\max} \le F_{ij,s,t} \le y_{ij,s,t}F_l^{\max} \\ -y_{ij,s,t}F_l^{\max} \le Q_{ij,s,t} \le y_{ij,s,t}F_l^{\max}, \end{cases} \quad \forall (i,j) \in \Omega_L \quad \forall t \in [1,T] \quad \forall s \in [1,N_s] \quad (16)$$

$$\begin{aligned} &-F_{ij}^{\max}\big(1 - y_{ij,s,t}\big) \le F_{ij,s,t} - \Big(G_{ij}V_{j,s,t} - B'_{ij}\theta_{j,s,t}\Big) \le F_{ij}^{\max}\big(1 - y_{ij,s,t}\big), \\ &-F_{ij}^{\max}\big(1 - y_{ij,s,t}\big) \le Q_{ij,s,t} - \Big(B_{ij}V_{j,s,t} - G'_{ij}\theta_{j,s,t}\Big) \le F_{ij}^{\max}\big(1 - y_{ij,s,t}\big), \\ &\forall (i,j) \in \Omega_L \quad \forall t \in [1,T] \quad \forall s \in [1,N_s] \end{aligned} \quad (17)$$

Note that the partial active and reactive load curtailments $\Delta P_{L,j,s,t}$ and $\Delta Q_{L,j,s,t}$ are restricted by

$$\begin{cases} 0 \le \Delta P_{L,j,s,t} \le P_{L,j,t}^0 \\ 0 \le \Delta Q_{L,j,s,t} \le Q_{L,j,t}^0, \end{cases} \quad \forall j \in \Omega_N \quad \forall t \in [1,T] \quad \forall s \in [1,N_s] \quad (18)$$

3) Generator Dispatch Constraint: The generation dispatch of a committed unit is limited by its generation capacity (i.e., $P_{G,i,t}^{min}$ and $P_{G,i,t}^{max}$ for active power; $Q_{G,i,t}^{min}$ and $Q_{G,i,t}^{max}$ for reactive power). Thus, the generation dispatch constraint is expressed as

$$x_{G,i,t}P_{G,i}^{\min} \le P_{G,i,s,t} \le x_{G,i,t}P_{G,i}^{\max}, \quad \forall i \in \Omega_G \quad \forall t \in [1,T] \quad \forall s \in [1,N_s] \quad (19)$$

$$x_{G,i,t}Q_{G,i}^{\min} \le Q_{G,i,s,t} \le x_{G,i,t}Q_{G,i}^{\max}, \quad \forall i \in \Omega_G \quad \forall t \in [1,T] \quad \forall s \in [1,N_s] \quad (20)$$

4) Generator Ramping Rate Constraint: The ramping of the i-th generator, which is not affected by typhoon, is limited by allowable upward $R_{G,i}^U$ and downward $R_{G,i}^D$ rates. A generation unit that is in the typhoon area will not be dispatched

due to possible communication outages. Hence, the ramping rate constraint is written as

$$P_{G,i,s,t+1} - P_{G,i,s,t} \le R^{U}_{G,i,t} x_{G,i,t} + P^{\min}_{G,i} v_{G,i,t+1}, \quad \forall i \in \Omega_G \backslash \Omega_B(s,t), \forall t \in [1,T], \forall s \in [1,N_s] \tag{21}$$

$$P_{G,i,s,t} - P_{G,i,s,t+1} \le R^{D}_{G,i,t} x_{G,i,t} + P^{\min}_{G,i} w_{G,i,t+1}, \quad \forall i \in \Omega_G \backslash \Omega_B(s,t) \quad \forall t \in [1,T] \quad \forall s \in [1,N_s] \tag{22}$$

$$-P^{\min}_{G,i} w_{G,i,t+1} \le P_{G,i,s,t+1} - P_{G,i,s,t} \le P^{\min}_{G,i} v_{G,i,t+1}, \quad \forall i \in \Omega_B(s,t) \quad \forall t \in [1,T] \quad \forall s \in [1,N_s] \tag{23}$$

5) Generator Up/Down Time Constraint: Each generator needs the minimum up/down time to start up or shut down due to the physical limit, which is ensured by

$$\sum_{k=t-T^{UP}_{G,i}}^{t} v_{G,i,k} \le x_{G,i,t}, \quad \sum_{k=t-T^{DN}_{G,i}}^{t} w_{G,i,k} \le 1 - x_{G,i,t}, \quad \forall i \in \Omega_G \quad \forall t \in \left[T^{UP}_{G,i}+1, T\right] \tag{24}$$

where $T^{UP}_{G,i}$ and $T^{DN}_{G,i}$ are the minimum time for startup and shutdown of unit i, respectively.

6) Spinning Reserve Constraint: The spinning reserve at time t for s-th path (i.e., $P^{R}_{s,t}$) can be expressed as the total capacity of generators minus the total load demand:

$$P^{R}_{s,t} = \sum_{\forall i \in \Omega_G} x_{G,i,t} P^{\max}_{G,i,t} - \sum_{\forall j \in \Omega_N} \left(P^{0}_{L,j,t} - \Delta P_{L,j,s,t}\right), \quad \forall t \in [1,T] \quad \forall s \in [1,N_s] \tag{25}$$

To cope with the typhoon in area $\Omega_A(s,t)$, the spinning reserve is considered to be larger than either the largest generation capacity, or a certain percent of total load demand with α_{re}, such that

$$P^{R}_{s,t} \ge \max\left[\max_{\forall i \in \Omega_G \bigcap \Omega_A(s,t)} \left(P^{\max}_{G,i}\right), \alpha_{\text{re}} \sum_{\forall j \in \Omega_N \bigcap \Omega_A(s,t)} \left(P^{0}_{L,j,t} - \Delta P_{L,j,s,t}\right)\right], \quad \forall t \in [1,T] \quad \forall s, \in [1,N_s] \tag{26}$$

7) Resource Management Constraint: Let a binary variable $r_{l,s,t}$ denote the time for starting the repair for s-th path. Specifically, $r_{l,s,t} = 1$ if the damaged transmission line l starts to be repaired at time t for s-th path; otherwise $r_{l,s,t} = 0$. Note that any damaged transmission line is repaired at most once, given by

$$\sum_{k=1}^{t} r_{l,s,k} \le 1 \quad \forall l \in \Omega_L \quad \forall t \in [1,T] \quad \forall s \in [1,N_s] \tag{27}$$

In particular, the lines outside the area $\Omega^{l}_{C}(s,t)$ are not subject to any repairs, which is stated as

$$r_{l,s,t} = 0 \quad \forall l \in \Omega^{l}_{A}(s,t) \bigcap \Omega^{l}_{B}(s,t) \bigcap \Omega_L, \quad \forall t \in [1,T] \quad \forall s \in [1,N_s] \tag{28}$$

The number of transmission lines that can be repaired simultaneously is limited by available resources, given by

$$\sum_{ij \in \Omega_L} z_{l,s,t} \le X \quad \forall t \in [1,T] \quad \forall s \in [1,N_s] \tag{29}$$

where X is the line repair limit.

TABLE II
DETAILED FORMULATION OF THE PROPOSED MODEL

Optimization Model		Equations
Objective		(2)-(4), (6)-(7)
Constraint sets	① logic constraint	(8)
	② power flow constraint	(9)-(18)
	③ generator dispatch constraint	(19)-(20)
	④ generator ramping rate constraint	(21)-(23)
	⑤ generator up/down time constraint	(24)
	⑥ spinning reserve constraint	(25)
	⑦ resource management constraint	(26)
	⑧ linearization constraint for the objective	(5)

A line repair is done within a certain number of periods. Thus, the $r_{l,s,t}$ and $z_{l,s,t}$ relationship is expressed as

$$\sum_{k=t-T^{REP}_{l}}^{t} r_{l,s,k} = z_{l,s,t} \quad \forall l \in \Omega_L, \quad \forall t \in [T^{REP}_{l}+1, T], \forall s \in [1,N_s] \tag{30}$$

where T^{REP}_{l} represents the total number of periods for line l repair. For special periods when $t = T^{REP}_{l}$, the logic constraints on $r_{l,s,t}$ and $z_{l,s,t}$ are reformulated as

$$\sum_{k=1}^{t} r_{l,s,k} = z_{l,s,t} \quad \forall l \in \Omega_L \quad \forall t \in \left[1, T^{REP}_{l}\right] \quad \forall s \in [1,N_s] \tag{31}$$

Furthermore, this model assumes that no repair is scheduled at the end of the period which cannot be completed within the allowable time. Accordingly,

$$z_{l,s,t} = 0 \quad \forall l \in \Omega_L \quad \forall t \in [T - T^{REP}_{l} + 1, T] \quad \forall s \in [1,N_s] \tag{32}$$

Finally, according to the forecast, a preset parameter $y^{0}_{l,t}$ is employed to characterize the line l outage caused by the occurrence of typhoon at time t. If a transmission line is on outage at time t, then $y^{0}_{l,t} = 1$ for all periods before the time t and $y^{0}_{l,t} = 0$ for all periods after time t.

It is intuitive that line l would be repaired only if it is damaged, which gives a logic relationship between $z_{l,s,t}$ and $y^{0}_{l,t}$ for the line l at the time t, such that

$$z_{l,s,t} \le 1 - y^{0}_{l,t} \quad \forall l \in \Omega_L \quad \forall t \in [1,T] \quad \forall s \in [1,N_s] \tag{33}$$

When the line l is damaged by the typhoon, it will be repaired after the typhoon is concluded. Thus, the relationship among $y^{0}_{l,t}$, $y_{l,s,t}$, and $r_{l,s,t}$ will satisfy

$$y_{l,s,t} = y^{0}_{l,t} + \sum_{k=1}^{t-T^{REP}_{l}} r_{l,s,k}, \quad \forall l \in \Omega_L \quad \forall t \in \left[T^{REP}_{l}, T\right] \quad \forall s \in [1,N_s] \tag{34}$$

Finally, the detailed formulation of the proposed optimization model can be expressed in Table II.

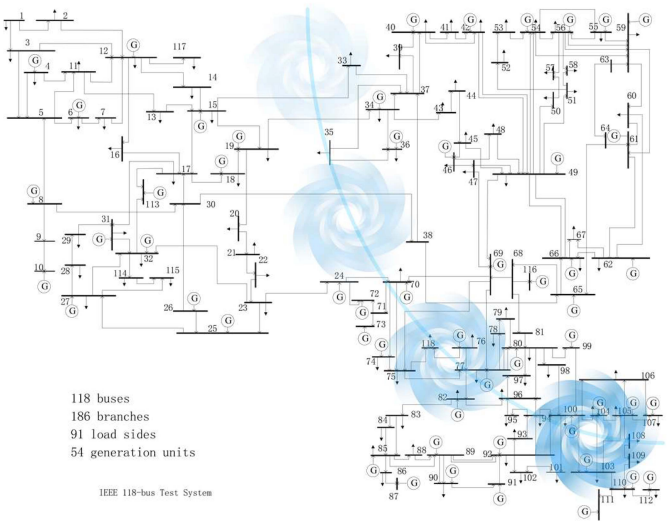

Fig. 3. Typhoon path in the IEEE 118-bus system.

TABLE III
GENERATOR CAPACITIES AND TYPES

Bus No. for Units	Type	Pmax (MW)	Ramp (MW/h)
33, 41, 46, 49	Oil	20	20
1, 2, 3, 6, 8, 9, 12, 13, 15, 17, 18, 31, 32, 38	Oil	30	30
42, 50, 54	Gas	50	25
30	Gas	80	40
7, 14, 16, 19, 22, 23, 26, 34, 35, 37, 47, 48, 51, 52, 53	Gas	100	50
24, 25, 40	Coal	200	60
20, 21	Coal	250	75
4, 5, 10, 29, 36, 39, 43, 44, 45	Coal	300	90
11	Coal	350	105
27, 28	Coal	420	126

III. CASE STUDY

We used a modified IEEE 118-bus system [33] and a real-world provincial power grid to verify the effectiveness of the proposed model. The proposed model was carried out using Python 3.6 on a workstation with an eight-thread 3.60-GHz CPU and 16.0 GB RAM memory. The mixed-integer linear programming was solved by GUROBI commercial solver with a gap of 0.1%.

A. Modified IEEE 118-Bus System

Consider a typhoon in the modified IEEE 118-bus system with a forecasted moving path. We acknowledge that there may be considerable uncertainties in the storm path and evolution. To address this problem, we assume all transmission lines located in the typhoon path are on outage and cascade sequentially. The system topology with the forecasted typhoon path is shown in Fig. 3. There are 118 buses (including 91 load nodes), 186 branches, and 54 generators in the system. Since different units may have different ramp rate capabilities, the generators are divided into three fuel types including oil, gas, and coal, with the corresponding generation capacities listed in Table III. Oil and gas-fired units have smaller capacities than those of coal-fired units, but possess faster startup and shutdown responses to provide power support in typhoons.

TABLE IV
DAMAGED LINES DURING A TYPHOON

Period	Branch(es)
5	177, 175, 173, 170, 172, 169
6	166, 171, 168, 165, 174, 176
7	164, 167, 163, 160, 159, 158
8	153, 154, 155, 145, 150, 148, 152
9	144, 146, 147, 151, 127
10	126, 125, 125, 123, 157, 156, 149
11	122, 121, 118, 128, 96
12	116, 186, 185, 120, 129, 108
13	115, 114, 117, 110, 112, 113, 109, 111, 30
15	54
17	46, 47
19	45
20	44

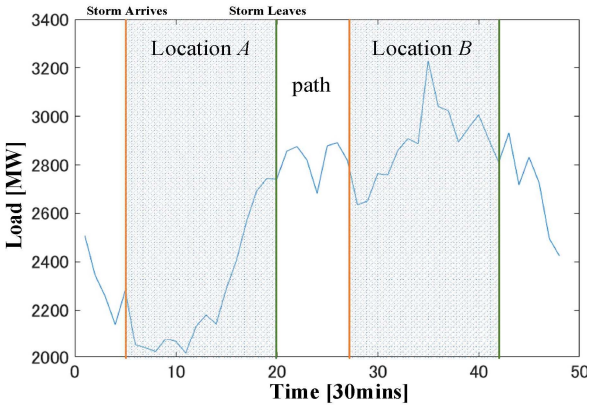

Fig. 4. Daily load profile.

In this example, cascaded transmission outages are shown in Table VI. The typhoon causes 62 transmission line outages which are actively repaired after the typhoon moves on. We assume eight lines can be repaired at the same time as resources are limited. Most line outages in a hurricane are due to flashovers caused by windage yaw. Each line requires 3 hours for flashover repair [39]–[40]. The model is conducted over 24 hours, and each time step is 30 minutes. The corresponding power outage cost is set approximately at 4,830 $/MWh. The daily system load profile is depicted in Fig. 4.

The three-stage resilient unit commitment schedule is shown in Fig. 5. Here, oil and gas-fired units (e.g., TG31, TG47) play an important role in the system response to typhoons. In this case, transmission line outages lead to load curtailments. Correspondingly, small-capacity gas and oil-fired generation units are started quickly to supply additional loads. For example, outages of two lines connected to bus 107 lead to the islanding of bus 107 whose loads will be supplied by TG49. The unit is started at 01:30 before the typhoon occurs. However, the TG49 capacity is only 20 MW, which cannot fully support the islanded load, so 3.75–6.9 MW of load is curtailed from 02:00 to 06:30 hours.

Similarly, the islanded bus 76 is supplied by the gas-fired unit TG34 which is started before the typhoon to prevent any load curtailments. In the meantime, TG45, which is a coal-fired unit, reduces its generation output gradually and is shut down before the typhoon arrives. This is because

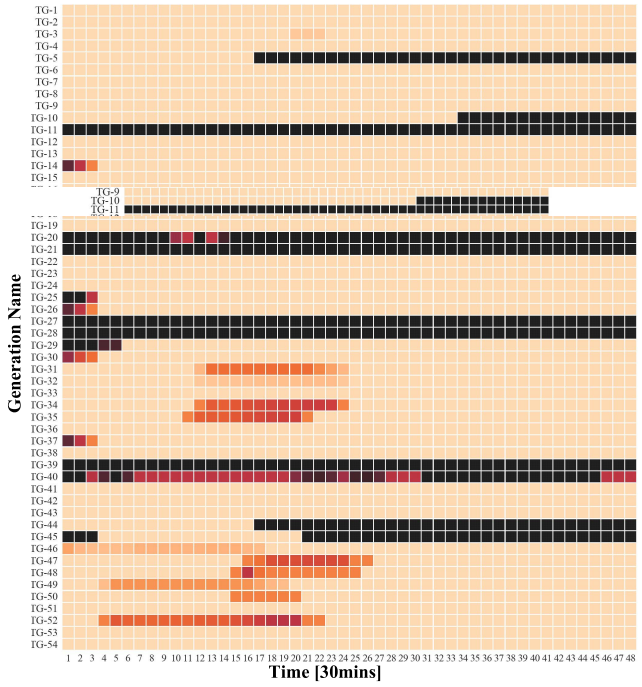

Fig. 5. Generation dispatch and unit commitment in typhoon.

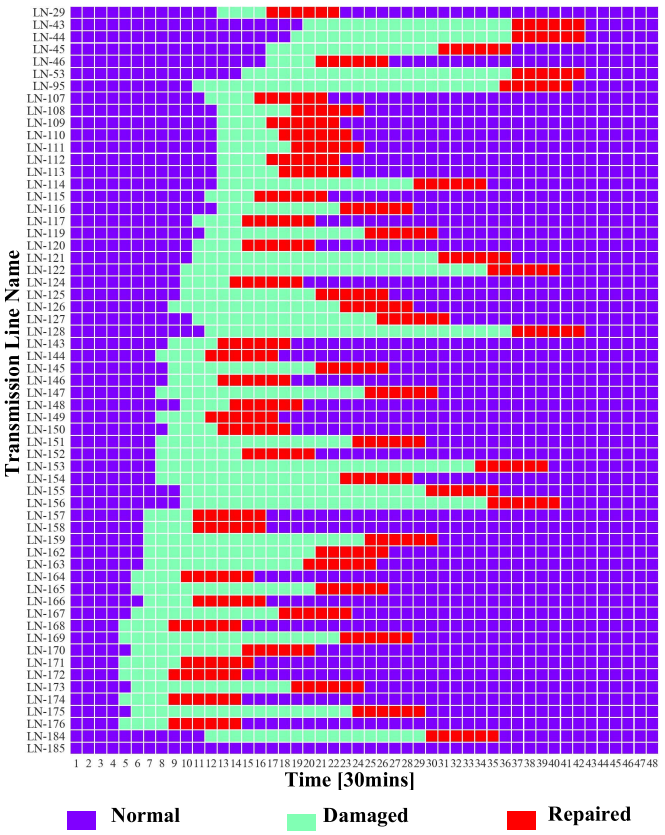

Fig. 6. States of lines in typhoon.

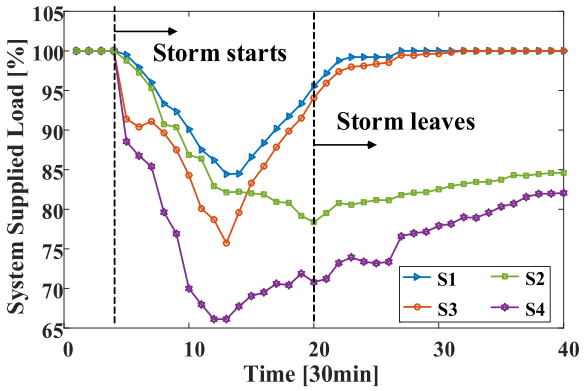

Fig. 7. Comparison of the resilience for four strategies.

the coal-fired unit has a slow-ramp generation output which cannot be adjusted quickly as evolving circumstances affect these buses. Relying solely on optimal generation unit scheduling might not be enough to improve the system resilience. The recovery to the normal operating state could also involve several transmission line repairs. Here, 62 lines are on outage during the typhoon and the optimal recovery sequence is presented in Fig. 6.

The repair priority depends on line outage contributions to load curtailments. Some lines are repaired shortly after they are on outage (e.g., LN176 and LN172), while others remain on outage for a longer time (e.g., LN95 and LN128). For example, three transmission lines (LN163, LN164, and LN167) connected to bus 104 are on outage. LN164 is repaired first, which will be connected to the power source at bus 103 to avoid any load curtailment. At that time, LN163 and LN167 are not significant because their recovery does not contribute to any load curtailment reductions; therefore, their priorities are relatively lower.

Furthermore, we design four strategies for comparison, denoted by S1-S4. S1 is the proposed method; S2 considers preventive control but neglects any line repairs in restoration, where loads are only restored by redispatch; S3 considers restoration while neglecting preventive control; S4 does not include either line maintenance or preventive control. Fig. 7 compares the resilience for four strategies, which resembles an upside down trapezoid. S4 shows the worst resilience case whereas S1 is the best strategy. The system load for S1 is curtailed sharply after the typhoon, but is quickly restored to its normal value by the coordination among flexible resources, including fast-start units and repair resources, which improves the power system resilience significantly. For S2, the pattern at the beginning is similar to that of S1 but the restoration is relatively slow when critically damaged lines are not repaired.

The number of lines that can be repaired at the same time depends on available resources. For example, if X repair groups can be dispatched where each group is allowed to repair one transmission line at the time, then X lines can be repaired at the same time. In order to investigate the impact of X on the performance of resilience solution, we design 3 cases where X is chosen as 6, 8, and 10, respectively and the results are shown in Fig. 8. Here, X will only affect the restoration stage without affecting prevention and emergency stages. The system will retain its normal status faster as X increases.

B. Provincial Power System

We choose a provincial power grid in China to study the impact of a typhoon on the system resilience. Here, transmission system voltages which are higher than 220 kV

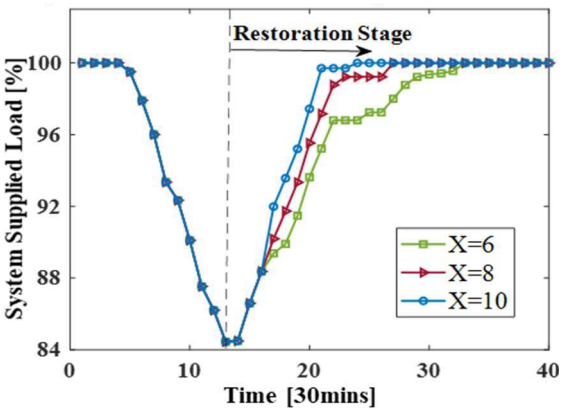

Fig. 8. System supplied load with X lines repaired simultaneously.

TABLE V
LINES ON OUTAGE FOLLOWING A TYPHOON PATH

Period	Lines
10	22-14,14-110,115-104
11	14-104,62-61,104-61,61-40,133-24
12	14-143,5-104,5-104,104-29,40-24,134-143
13	23-24,40-123,29-42,5-143
14	5-134,28-29,27-28
15	41-42,42-123,118-123,81-102,37-81
16	77-131,77-132,77-101,41-63,41-117
17	117-118,31-84,84-125,31-125,63-117
18	114-118,118-119,31-43,30-31,30-46,43-70
20	70-85,70-113,70-74,47-74,74-86,10-46
22	10-47,98-141,19-98,99-142
23	19-99,19-21,119-120,120-121
24	19-121,19-13,19-18,13-9,18-9,9-10,9-10

and correspond to 144 buses, 178 transmission lines, and 35 generation units are considered in Fig. 8. There are 30 coal-fired units, which have slow ramp rates; 5 gas-fired units, which can ramp up from minimum to maximum in 1 hour; and 9 oil-fired units, which can ramp from minimum to maximum in 30 minutes. The cascaded outages of 63 transmission lines are presented in Table V, which account for 35.4% of the total number of transmission lines.

The additional gas-fired (G33) and oil-fired units (G37, G39, G40, G43, and G44) with their fast-start flexibility can actively provide 1582.31 MWh to prevent significant load curtailments. Take G40 for example. As the typhoon approaches, G40 is started to provide a 220-MW of power supply. During the typhoon, lines (104-29, 29-42, and 29-28) will be on outage which lead bus 29 to become an island, while G40 continues to provide its supply as lines are being repaired. The coal-fired units also can contribute to the generation supply during the typhoon. Unit G4 is operated at its maximum output (i.e., 1320 MW) in the 18th period which is decreased after the 19th period. The power output is reduced to its minimum (i.e., 792 MW) at the 21th period and is shut down at the 22th period, which is one hour before the typhoon hits. After the typhoon, the line which feeds G4 is under repair during the 32th period as the unit is started at its minimum output. When this line is completely repaired, unit G4 output will be increased to its maximum.

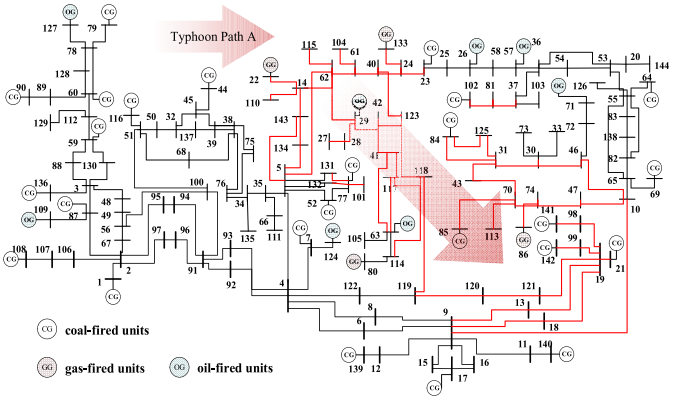

Fig. 9. Topology of the provincial power system and the typhoon Path.

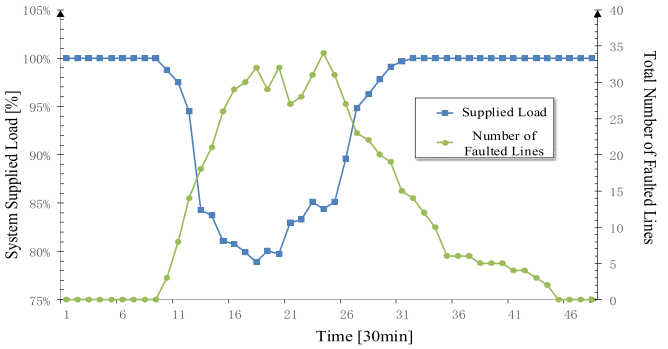

Fig. 10. Lines on outage and system load profile.

The proper strategy for repairing the damaged lines can also help restore loads quickly and improve resilience. At the 11th period, five lines (14-104, 62-61, 104-61, 61-40, and 133-24) are on outage simultaneously, but their repairs are done sequentially. The critical lines (14-104, 62-61, 61-40, and 133-24) are repaired 2 hours after the typhoon, but line 104-61 which is less critical, is not repaired until the 23th period. Similarly, in the 17th period, lines (117-118, 31-84, 84-125, 31-125, and 63-117) trip simultaneously. In this case, two lines (117-118 and 63-117) are less critical because the repaired line 41-117 will recover 800 MW, which can satisfy a 345-MW load. This means the two lines are redundant.

Fig. 10 depicts the supplied load profile and lines on outage during the typhoon. Here, the load curtailment occurs after the 10th period. During the 10th through the 13th periods, lines cannot be repaired and the system recovers against the typhoon only by using gas and oil-fired units. At this time, the load shedding is increased quickly to 15.75%. After the 14th period, a few lines are repaired and the coal-fired units (G26 and G9) are started, so the load curtailment is slowed down. Until the 18th period, when load curtailment reaches 21.13%, the load will be recovered gradually. During the load recovery, the load curtailment is decreased to 19.96% in the 19th period and then increased to 20.27% in the 20th period. This is because line 6 is on outage during the 20th period which leads to an additional 0.31% load curtailment. Furthermore, during the 31th period (i.e., 3 hours after the typhoon has moved on) the load is recovered to 99.68%, although 15 lines are still on outage.

TABLE VI
LINE OUTAGES IN THE TWO SCENARIOS FOR THE THREE TYPHOON PATHS

Periods	Path A		Path B		Path C	
	Mild damage	Moderate damage	Mild damage	Moderate damage	Mild damage	Moderate damage
10	115-104	14-110,115-104	115-104	14-110,115-104	115-104	14-110,115-104
11	14-104,61-40	14-104,61-40,133-24	14-104,61-40	14-104,61-40,133-24	14-104,61-40	14-104,61-40,133-24
12	104-29,40-24	5-104, 104-29,40-24	104-29,40-24	5-104, 104-29,40-24	104-29,40-24	5-104, 104-29,40-24
13	40-123,29-42	40-123,29-42,5-143	40-123,29-42	40-123,29-42,5-143	40-123,29-42	40-123,29-42,5-143
14	28-29,27-28	5-134,28-29,27-28	28-29,27-28	5-134,28-29,27-28	28-29,27-28	5-134,28-29,27-28
15	42-123,118-123	41-42,42-123,118-123	42-123,5-131	42-123,5-131,5-132	102-81,81-37	102-81,81-37
16	77-101,41-63,41-117	77-101,41-63,41-117	77-101,41-63,41-117	77-101,41-63,41-117	23-25,41-117	23-25,41-117,77-131
17	117-118, 63-117	31-84,31-125,63-117	5-52,52-77	5-52,52-77,7-124	37-54,84-125	37-54,84-125,31-125
18	118-119,31-43	118-119,31-43,30-46	4-7,63-105	4-7,63-105,114-80	31-125,71-72	31-125,114-118,71-72
20	70-85,70-113,74-86	70-85,70-113,70-74, 74-86	4-122,4-8,6-8	4-122,4-8,6-8,9-12,6-9	72-46,37-103	72-46,37-103,30-33,30-46
22	98-141 ,99-142	98-141,19-98,99-142	12-139,15-17	12-139,15-17,17-16	83-138,82-65	83-138,82-138,82-65
23	19-99,120-121	19-99,19-21,120-121	/	/	/	/
24	19-121,19-13,19-18	19-121,19-13,19-18,9-10	/	/	/	/

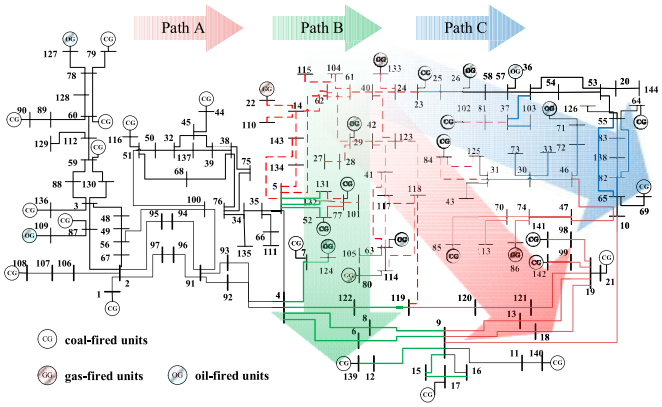

Fig. 11. Three typhoon path predictions.

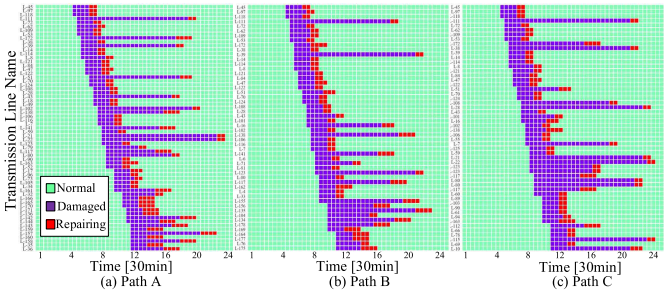

Fig. 12. Line states in the three typhoon path predictions.

TABLE VII
LOAD CURTAILMENTS IN DAMAGE SCENARIOS

Paths	Mild damage (GWh)		Moderate damage (GWh)		Serious damage (GWh)	
	P1	P2	P1	P2	P1	P2
Path A	3.22	5.34	4.08	5.02	4.80	4.80
Path B	1.45	2.77	1.98	2.57	2.39	2.39
Path C	2.26	3.52	2.68	3.36	2.98	2.98

TABLE VIII
PENALTY COST FOR DAMAGE SCENARIOS

Paths	Mild damage (Million $)		Moderate damage (Million $)		Serious damage (Million $)	
	P1	P2	P1	P2	P1	P2
Path A	34.85	36.46	35.50	36.22	36.05	36.05
Path B	33.50	34.51	33.90	34.35	34.22	34.22
Path C	34.12	35.08	34.44	34.95	34.66	34.66

The proposed three-stage resilient unit commitment can provide pre-arranged plans for typhoon paths, including the dispatching of the quick-start units and the strategy for line repairs. A typhoon may pose several paths considering the event parameters (e.g., weather, geographical conditions, time of the year, etc.). Accordingly, we deploy a stochastic model in which we consider several pre-defined plans for all possible typhoon paths and their corresponding probabilities. Assume that there are three predicted typhoon paths across three different areas as depicted in Fig. 11. For each possible typhoon path, we assume all possible lines are on outage to manifest the worst case and seek a robust solution. The line states in the three paths are shown in Fig. 12, which indicate the line outages during the typhoon and repair status after the typhoon. The dispatchers can track the typhoon paths for each plan and make viable decisions when the corresponding typhoon path occurs in real-time.

The above analyses are carried out by the proposed three-stage resilient unit commitment with multiple typhoon paths for the worst-case scenario in each path. To investigate the robustness of the proposed method, we consider more optimistic scenarios by assuming that certain lines in a typhoon path remain functional. Here, we design three scenarios in Table VI, including two optimistic scenarios and the worst-case scenario in each typhoon path, where 1) mild damage occurs when only the lines in the center of the typhoon path are damaged; 2) moderate damage occurs when lines in central areas and certain boundary lines are on outage in a typhoon path; 3) severe damage occurs when all lines in the typhoon path are on outage, i.e., the worst-case scenario.

We solve the proposed three-stage resilient unit commitment model with three possible paths representing mild, moderate, and serious damage scenarios, respectively. Simulation results are shown in Tables VII and VIII, where P1 represents the load curtailment of a certain path in the three-stage resilient unit commitment scheme, should the predicted damage level occurs; P2 represents the load curtailment in the

TABLE IX
COMPUTATION TIMES OF STRATEGIES S1-S4

		Continuous Variables	Binary Variables	Constraints	Time (min)
IEEE 118-bus System	S1	22848	34560	92388	22
	S2	22848	16704	56256	8
	S3	21984	31968	86340	21
	S4	21984	15840	50208	6
Provincial System	S1	24480	33864	97632	27
	S2	24480	16776	63246	10
	S3	23466	31848	88274	26
	S4	23466	14760	57288	9

worst-case scenario, where the three-stage resilient unit commitment scheme was based on the current prediction. If the predicted outage occurs, the load curtailment will increase as the outage level progresses from mild to worst (i.e., load curtailment in Path A increases from 3.22 GWh to 4.80 GWh, in Path B increases from 1.45 GWh to 2.39GWh, and in Path C increases from 2.26 GWh to 2.98GWh). Accordingly, the total cost in Path A increases from $ 34.85 million to $ 36.05 million, Path B from $ 33.50 million to $ 34.22 million, and Path C from $ 34.12 million to $ 34.66 million.

However, if the worst-case scenario occurs, the dispatch plan based on mild, moderate, and severe damage predictions will cause additional 2.12GWh (65.8%), 0.94GWh (23.1%) and 0 GWh (0%) load curtailments, respectively. Accordingly, the additional cost saving will be $1.61 million (4.6%), $0.71 million (2.1%) and $0 million (0%), respectively. This means the proposed model considering the worst-case scenario is more robust than other proposed strategies, saving 0.54 GWh and 0.22 GWh for mild and moderate damages, respectively; and saving $0.41 million and $ 0.17 million for mild and moderate damages, respectively. Therefore, once the worst-case scenario occurs, the load will be curtailed more using the optimistic strategies, whereas the proposed three-stage resilient unit commitment can reduce the load curtailment and the total operation cost.

Finally, the computation time for the four strategies S1-S4 can be found in Table IX. The proposed model S1 contains the most numbers of variables and constraints, so the computation time is longest. Generally, it needs about 20-30 minutes to solve two test systems. Strategy S4 is fastest because this model neglects either line maintenance or preventive control, containing the least numbers of variables and constraints. However, the proposed model is a day-ahead unit commitment for pre-arranged plans which doesn't aim to use for real-time applications, so the algorithm complexity is not as critical as the real-time applications. Half-hour computation time can meet the requirement of the day-ahead dispatch.

IV. CONCLUSION

This article has set up a three-stage resilient unit commitment model considering the stochasticity of typhoon paths and line outages to improve the power systems resilience during typhoons. The simulation results on the IEEE 118-bus system and a real-world provincial power system show that the proposed three-stage resilient unit commitment can coordinate control strategies for the three stages, enabling the power system to reduce the load curtailment throughout the entire dynamic process. Moreover, fast-start units can be committed in advance to prevent load shedding under possible contingencies and critical line repairs are initiated immediately to pick up critical loads as quickly as possible. Future work will incorporate dynamic system simulations into the proposed three-stage resilient unit commitment.

REFERENCES

[1] P.-Y. Liu, H.-M. He and C.-P .Pan, "Investigation of 2008' frozen disaster and research on de-icing in Guangdong power grid," in *Proc. China Int. Conf. Elect. Distrib.*, Guangzhou, China, 2008, pp. 1–5.

[2] T. Majima, D. Watanabe, K. Takadama, and M. Katuhara, "Support system for transportation under disaster circumstance," in *Proc. SICE Annu. Conf.*, Tokyo, Japan, 2011, pp. 137–142.

[3] G. Liang, S. R. Weller, J. Zhao, F. Luo, and Z. Y. Dong, "The 2015 Ukraine blackout: Implications for false data injection attacks," *IEEE Trans. Power Syst.*, vol. 32, no. 4, pp. 3317–3318, Jul. 2017.

[4] H. Hui, Y. Ding, K. Luan, and D. Xu, "Analysis of '8•15' blackout in Taiwan and the improvement method of contingency reserve capacity through direct load control," in *Proc. IEEE Power Energy Soc. Gen. Meeting*, Portland, OR, USA, 2018, pp. 1–5.

[5] H. H. Alhelou, M. E. Hamedani-Golshan, T. C. Njenda, and P. Siano, "A survey on power system blackout and cascading events: Research motivations and challenges," *Energies*, vol. 12, no. 4, pp. 1–28, 2019.

[6] P. E. Roege, Z. A. Collier, J. Mancillas, and I. Linkov, "Metrics for energy resilience," *Energy Policy*, vol. 72, no. 1, pp. 249–256, Sep. 2014.

[7] Z. Li, M. Shahidehpour, F. Aminifar, A. Alabdulwahab, and Y. Al-Turki, "Networked microgrids for enhancing the power system resilience," *Proc. IEEE*, vol. 105, no. 7, pp. 1289–1310, Jul. 2017.

[8] J. W. Muhs and M. Parvania, "Stochastic spatio-temporal hurricane impact analysis for power grid resilience studies," in *Proc. IEEE Innov. Smart Grid Technol. (ISGT) Conf.*, Washington, DC, USA, Feb. 2019, pp. 1–5.

[9] X. Wang, M. Shahidehpour, C. Jiang, and Z. Li, "Resilience enhancement strategies for power distribution network coupled with urban transportation system," *IEEE Trans. Smart Grid*, vol. 10, no. 4, pp. 4068–4079, Jul. 2019.

[10] B. Falahati, Y. Fu, and L. Wu, "Reliability assessment of smart grid considering direct cyber-power interdependencies," *IEEE Trans. Smart Grid*, vol. 3, no. 3, pp. 1515–1524, Sep. 2012.

[11] C. Chen, J. Wang, F. Qiu, and D. Zhao, "Resilient distribution system by microgrids formation after natural disasters," *IEEE Trans. Smart Grid*, vol. 7, no. 2, pp. 958–966, Mar. 2016.

[12] G. Huang, J. Wang, C. Chen, J. Qi, and C. Guo, "Integration of preventive and emergency responses for power grid resilience enhancement," *IEEE Trans. Power Syst.*, vol. 32, no. 6, pp. 4451–4463, Nov. 2017.

[13] Y. Liu, Q. H. Wu, and X. X. Zhou, "Co-ordinated multiloop switching control of DFIG for resilience enhancement of wind power penetrated power systems," *IEEE Trans. Sustain. Energy*, vol. 7, no. 3, pp. 1089–1099, Jul. 2016.

[14] C. Shao, M. Shahidehpour, X. Wang, X. Wang, and B. Wang, "Integrated planning of electricity and natural gas transportation systems for enhancing the power grid resilience," *IEEE Trans. Power Syst.*, vol. 32, no. 6, pp. 4418–4429, Nov. 2017.

[15] Y. Dai *et al.*, "Integrated dispatch model for combined heat and power plant with phase-change thermal energy storage considering heat transfer process," *IEEE Trans. Sustain. Energy*, vol. 9, no. 3, pp. 1234–1243, Jul. 2018.

[16] T. Ding, M. Qu, X. Wu, B. Qin, Y. Yang, and F. Blaabjerg, "Defense strategy for resilient shipboard power systems considering sequential attacks," *IEEE Trans. Inf. Forensics Security*, vol. 15, pp. 3443–3453, Dec. 2019.

[17] R. Nateghi, "Multi-dimensional infrastructure resilience modeling: An application to hurricane-prone electric power distribution systems," *IEEE Access*, vol. 6, pp. 13478–13489, 2018.

[18] A. Shahsavari, M. Farajollahi, E. M. Stewart, E. Cortez, and H. Mohsenian-Rad, "Situational awareness in distribution grid using micro-PMU data: A machine learning approach," *IEEE Trans. Smart Grid*, vol. 10, no. 6, pp. 6167–6177, Nov. 2019.

[19] C. Wang, Y. Hou, F. Qiu, S. Lei, and K. Liu, "Resilience enhancement with sequentially proactive operation strategies," *IEEE Trans. Power Syst.*, vol. 32, no. 4, pp. 2847–2857, Jul. 2017.
[20] M. Panteli, C. Pickering, S. Wilkinson, R. Dawson, and P. Mancarella, "Power system resilience to extreme weather: Fragility modeling, probabilistic impact assessment, and adaptation measures," *IEEE Trans. Power Syst.*, vol. 32, no. 5, pp. 3747–3757, Sep. 2017.
[21] M. Yan *et al.*, "Enhancing the transmission grid resilience in ice storms by optimal coordination of power system schedule with pre-positioning and routing of mobile DC de-icing devices," *IEEE Trans. Power Syst.*, vol. 34, no. 4, pp. 2663–2674, Jul. 2019.
[22] Y. Chi, Y. Xu, and T. Ding, "Coordinated VAR planning for voltage stability enhancement of a wind-energy power system considering multiple resilience indices," *IEEE Trans. Sustain. Energy*, vol. 11, no. 4, pp. 2367–2379, Oct. 2020.
[23] W. Sun, C.-C. Liu, and L. Zhang, "Optimal generator start-up strategy for bulk power system restoration," *IEEE Trans. Power Syst.*, vol. 26, no. 3, pp. 1357–1366, Aug. 2011.
[24] S. Toune, H. Fudo, T. Genji, Y. Fukuyama, and Y. Nakanishi, "Comparative study of modern heuristic algorithms to service restoration in distribution systems," *IEEE Trans. Power Del.*, vol. 17, no. 1, pp. 173–181, Jan. 2002.
[25] C. Wang, P. Ju, S. Lei, Z. Wang, F. Wu, and Y. Hou, "Markov decision process-based resilience enhancement for distribution systems: An approximate dynamic programming approach," *IEEE Trans. Smart Grid*, vol. 11, no. 3, pp. 2498–2510, May 2020.
[26] S. Ma, B. Chen, and Z. Wang, "Resilience enhancement strategy for distribution systems under extreme weather events," *IEEE Trans. Smart Grid*, vol. 9, no. 2, pp. 1442–1451, Mar. 2018.
[27] S. Ma, L. Su, Z. Wang, F. Qiu, and G. Guo, "Resilience enhancement of distribution grids against extreme weather events," *IEEE Trans. Power Syst.*, vol. 33, no. 5, pp. 4842–4853, Sep. 2018.
[28] B. Chen, Z. Ye, C. Chen, J. Wang, T. Ding, and Z. Bie, "Toward a synthetic model for distribution system restoration and crew dispatch," *IEEE Trans. Power Syst.*, vol. 34, no. 3, pp. 2228–2239, May 2019.
[29] S. Ma, S. Li, Z. Wang, and F. Qiu, "Resilience-oriented design of distribution systems," *IEEE Trans. Power Syst.*, vol. 34, no. 4, pp. 2880–2891, Jul. 2019.
[30] T. Ding, Y. Lin, G. Li, and Z. Bie, "A new model for resilient distribution systems by microgrids formation," *IEEE Trans. Power Syst.*, vol. 32, no. 5, pp. 4145–4147, Sep. 2017.
[31] Z. Wang and J. Wang, "Self-healing resilient distribution systems based on sectionalization into microgrids," *IEEE Trans. Power Syst.*, vol. 30, no. 6, pp. 3139–3149, Nov. 2015.
[32] T. Ding, Y. Lin, Z. Bie, and C. Chen, "A resilient microgrid formation strategy for load restoration considering master-slave distributed generators and topology reconfiguration," *Appl. Energy*, vol. 199, pp. 205–216. Aug. 2017.
[33] J. Aghaei and M. I. Alizadeh, "Robust n–k contingency constrained unit commitment with ancillary service demand response program," *IET Gen. Transm. Distrib.*, vol. 8, no. 12, pp. 1928–1936, 2014.
[34] A. Street, F. Oliveira, and J. M. Arroyo, "Contingency-constrained unit commitment with *N-k* security criterion: A robust optimization approach," *IEEE Trans. Power Syst.*, vol. 26, no. 3, pp. 1581–1590, Aug. 2011.
[35] Q. Wang, J. Watson, and Y. Guan, "Two-stage robust optimization for *N–k* contingency-constrained unit commitment," *IEEE Trans. Power Syst.*, vol. 28, no. 3, pp. 2366–2375, Aug. 2013.
[36] D. Pozo and J. Contreras, "A chance-constrained unit commitment with an *n–K* security criterion and significant wind generation," *IEEE Trans. Power Syst.*, vol. 28, no. 3, pp. 2842–2851, Aug. 2013.
[37] C. Zhao and R. Jiang, "Distributionally robust contingency-constrained unit commitment," *IEEE Trans. Power Syst.*, vol. 33, no. 1, pp. 94–102, Jan. 2018.
[38] T. Zhao, H. Zhang, X. Liu, S. Yao, and P. Wang, "Resilient unit commitment for day-ahead market considering probabilistic impacts of hurricanes," *IEEE Trans. Power Syst.*, early access, Sep. 18, 2020, doi: 10.1109/TPWRS.2020.3025185.
[39] R. D. Zimmerman, C. E. Murillo-Sánchez, and R. J. Thomas, "MATPOWER: Steady-state operations, planning, and analysis tools for power systems research and education," *IEEE Trans. Power Syst.*, vol. 26, no. 1, pp. 12–19, Feb. 2011.
[40] A. Arif, Z. Wang, J. Wang, and C. Chen," "Power distribution system outage management with co-optimization of repairs, reconfiguration, and DG dispatch," *IEEE Trans. Smart Grid*, vol. 9, no. 5, pp. 4109–4118, Sep. 2018.
[41] A. Arif, S. Ma, and Z. Wang, "Optimization of transmission system repair and restoration with crew routing," in *Proc. North Amer. Power Symp. (NAPS)*, Denver, CO, USA, 2016, pp. 1–6.

Tao Ding (Senior Member, IEEE) received the B.S.E.E. and M.S.E.E. degrees from Southeast University, Nanjing, China, in 2009 and 2012, respectively, and the Ph.D. degree from Tsinghua University, Beijing, China, in 2015. From 2013 to 2014, he was a Visiting Scholar with the Department of Electrical Engineering and Computer Science, University of Tennessee, Knoxville, TN, USA. He is currently an Associate Professor with the State Key Laboratory of Electrical Insulation and Power Equipment, School of Electrical Engineering, Xi'an Jiaotong University. He has published more than 60 technical papers and authored by "Springer Theses" recognizing outstanding Ph.D. research around the world and across the physical sciences—*Power System Operation With Large-Scale Stochastic Wind Power Integration*. His current research interests include electricity markets, power system economics and optimization methods, and power system planning and reliability evaluation. He received the excellent master and doctoral dissertation from Southeast University and Tsinghua University, respectively, and the Outstanding Graduate Award of Beijing City. He is an Editor of IEEE TRANSACTIONS ON SMART GRID, IEEE POWER ENGINEERING LETTERS, *IET Generation Transmission & Distribution*, and *CSEE Journal of Power and Energy Systems*.

Ming Qu (Student Member, IEEE) received the B.S. degree from the School of Electrical Engineering, Shandong University, Jinan, China, in 2017. He is currently pursuing the Ph.D. degree with Xi'an Jiaotong University. His major research interests include power system optimization and renewable energy integration.

Zekai Wang (Student Member, IEEE) received the B.S. degree from the School of Electrical Engineering, Xi'an Jiaotong University, Xi'an, China, in 2018, where he is currently pursuing the M.S. degree. His major research interests include power system optimization and resilience.

Bo Chen (Member, IEEE) received the B.S. and M.S. degrees from North China Electric Power University, Baoding, China, and the Ph.D. degree in electrical engineering from Texas A&M University, College Station, USA, in 2017. In 2017, he worked as a Postdoctoral Researcher with Argonne National Laboratory, Lemont, IL, USA, where he is currently an Energy Systems Scientist with Energy Systems Division. His research interests include modeling, control, and optimization of power systems, cybersecurity, and cyber-physical systems.

Chen Chen (Senior Member, IEEE) received the B.S. and M.S. degrees from Xi'an Jiaotong University (XJTU), Xi'an, China, in 2006 and 2009, respectively, and the Ph.D. degree in electrical engineering from Lehigh University, Bethlehem, PA, USA, in 2013. He is currently a Professor with the School of Electrical Engineering, XJTU. Prior to joining XJTU, he has over six-year service with Argonne National Laboratory, Lemont, IL, USA, with the last appointment as an Energy Systems Scientist with Energy Systems Division. His research interests include power system resilience, distribution systems and microgrids, demand-side management, and communications and signal processing for smart grid. He is the recipient of the IEEE PES Chicago Chapter Outstanding Engineer Award in 2017. He is an Editor of IEEE TRANSACTIONS ON SMART GRID and IEEE POWER ENGINEERING LETTERS.

Mohammad Shahidehpour (Life Fellow, IEEE) received the Honorary Doctorate degree in electrical engineering from the Polytechnic University of Bucharest, Bucharest, Romania. He is the Bodine Chair Professor and the Director with the Robert W. Galvin Center for Electricity Innovation, Illinois Institute of Technology, Chicago, IL, USA. He is a Laureate of Khwarizmi International Award and an Elected Member of the U.S. National Academy of Engineering. He is listed as a Highly Cited Researcher on the Web Science (ranked in the top 1% by citations demonstrating significant influence among his peers). He is a Fellow of the American Association for the Advancement of Science and the National Academy of Inventors.